Biochemical and Biophysical Research Communications

Cytochrome C interacts with the pathogenic mutational hotspot region of TRPV4 and forms complexes that differ in mutation and metal ion-sensitive manner

--Manuscript Draft--

Manuscript Number:	BBRC-22-1612R1
Article Type:	Short communication/Research article
Keywords:	Cytochrome C, Metabolism, Ca2+, Channelopathy, Mitochondria
Corresponding Author:	Chandan Goswami, PhD National Institute of Science Education and Research Bhubaneswar, INDIA
First Author:	Rashmita Das
Order of Authors:	Rashmita Das
	Ashutosh Kumar
	Ritesh Dalai
	Chandan Goswami, PhD

Cover Letter

Dr. Chandan Goswami
Associate Professor
School of Biological Sciences, NISER
Ph : (0674) 2304044
e-mail : chandan@niser.ac.in
&
DAAD Research Ambassador, India
ra.goswami@daadindia.org

To

Prof. Wolfgang Baumeister
Editor-in-chief
Biochemical and Biophysical Research Communications

11th April 2022
NISER, Bhubaneswar

Sub: Submission of original article in the Biochemical and Biophysical Research Communications

Dear Sir,

Please find our manuscript entitled "**Cytochrome-C interacts with the pathogenic mutational hotspot region of TRPV4 and forms complexes that differ in mutation and metal ion-sensitive manner"** for publication in the Biochemical and Biophysical Research Communications. Collectively this manuscript demonstrates the following important points:

* TRPV4 interacts with Cytochrome C, a mitochondrial protein.
* This interaction is sensitive to different metal ions
* This interaction is mainly through a fragment of TRPV4 (i.e. TM4-Loop-TM5 region), a hot-spot for several mutations, which causes different diseases.
* Different mutants of TRPV4 interact with Cytochrome C differently.
* Collectively this finding can suggest for the role of TRPV4-Cytochroem C as a complex which is important for biological functions and that goes wrong in different mutations.

We believe that these findings are extremely novel and are relevant for several health-related disorders including TRPV4-mediated channelopathies. We hope that you will find this manuscript suitable for publication in the "Biochemical and Biophysical Research Communications".

Sincerely

Dr. Chandan Goswami

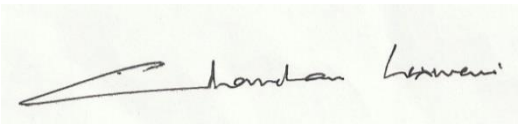

National Institute of Science Education and Research Bhubaneswar
P.O. Jatni, Khurda 752050, Odisha, India

Response to comments:

As per the suggestion, following changes were made

a) Figure 1, Figure 2 and Figure 4 has been reframed, reduced-in-size and/or content. Some of the contents (gel-based quantification) of Fig 1 and Fig are now placed as a supplementary figure 1. The respective figure legends have been reduced/edited accordingly.

b) The primer details now have been added as text and therefore the entire method section has been reduced a bit.

c) The typo error in the High-light section and in the main manuscript have been corrected.

High-light

* TRPV4 interacts with Cytochrome C
* This interaction is sensitive to different metal ions
* This interaction through the TM4-Loop-TM5 region of TRPV4
* The residues involved in this interaction are conserved throughout the vertebrates
* Different mutants of TRPV4 interact with Cytochrome C differently.
* TRPV4-Cytochrome C interaction might be relevant for TRPV4-mediated channelopathies

Graphical abstract

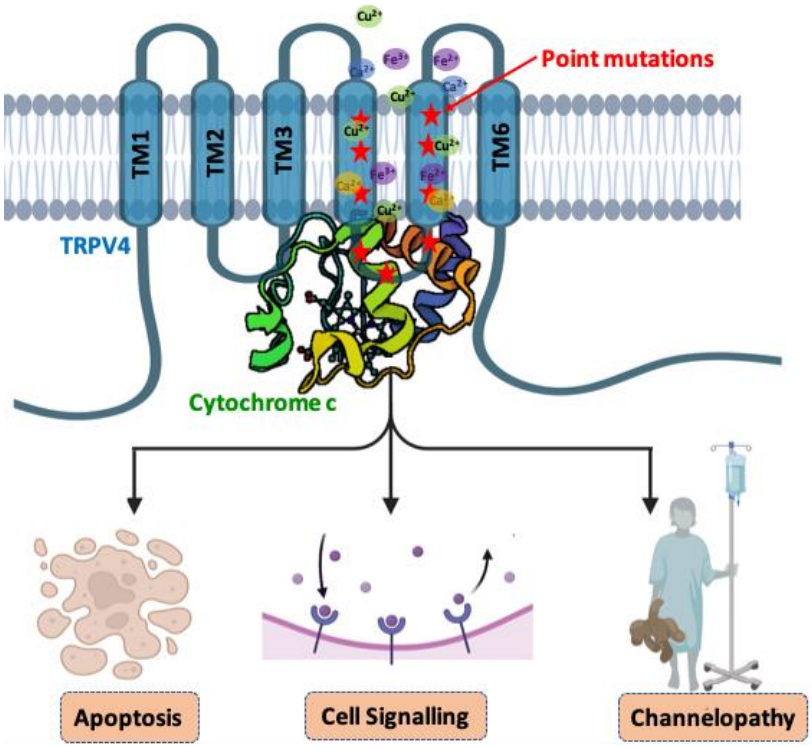

Cytochrome C interacts with TRPV4 in its mutational hotspot region. This interaction is different in presence of different metal ions and mutations. TRPV4-Cytochrome C complex can be relevant for apoptosis, cell signalling and different TRPV4-mediated channelopathies.

Cytochrome C interacts with the pathogenic mutational hotspot region of TRPV4 and forms complexes that differ in mutation and metal ion-sensitive manner

Rashmita Das[a, b,] Ashutosh Kumar[a,b], Ritesh Dalai [a,b], Chandan Goswami [a,b,*]

a: School of Biological Sciences, National Institute of Science Education and Research, HBNI, Khordha, Jatni, Odisha, 752050, India

b: Homi Bhabha National Institute, Training School Complex, Anushakti Nagar, Mumbai, 400094, India

* Correspondence: chandan@niser.ac.in

Abstract

The importance of TRPV4 in physiology and disease has been reported by several groups. Recently we have reported that TRPV4 localizes in the mitochondria in different cellular systems, regulates mitochondrial metabolism and electron transport chain functions. Here, we show that TRPV4 colocalizes with Cytochrome C (Cyt C), both in resting as well as in activated conditions. Amino acid region 592-630 of TRPV4 (termed as Fr592-630) that also covers TM4-Loop-TM5 region (which is also a hotspot of several pathogenic mutations) interacts with Cyt C, in a Ca^{2+}-sensitive manner. This interaction is also variable and sensitive to other divalent and trivalent cations (i.e., Cu^{2+}, Mn^{2+}, Ni^{2+}, Zn^{2+}, Fe^{3+}). Key residues of TRPV4 involved in these interactions remain conserved throughout the vertebrate evolution. Accordingly, this interaction is variable in the case of different pathogenic mutations (R616Q, F617L, L618P, V620I). Our data suggest that the TRPV4-Cyt C complex differs due to different mutations and is sensitive to the presence of different metal ions. We propose that TRPV4-Cyt C complex formation is important for physiological functions and relevant for TRPV4-induced channelopathies.

Key words: Cytochrome C, Metabolism, Ca^{2+}, Channelopathy, Mitochondria

Running title: Cytochrome C interaction with TRPV4

1. Introduction

TRPV4 is a non-selective cation channel that is expressed in several cells and tissues. Activation of TRPV4 results in influx of Ca^{2+} and other divalent cations. Importance of TRPV4 in different physiological and sensory functions are reported. So far a large number of missense variations of TRPV4 in human population have been identified [1]. While not all of these variations are not detrimental, there are several point mutations in TRPV4 have been identified that are pathogenic in nature [1]. However, all these mutations have different phenotypic penetration and the degree of pathology differs. Notably, many of these pathogenic mutations are located within the TM4-Loop-TM5 region, suggesting that these region act as a potential hotspot for TRPV4 structure-function and regulation [2]. Notably, the TM4-loop-TM5 region is critical for the channel function of TRPV4 too. Interestingly, the same region contains cholesterol-binding motif sequences which are highly conserved throughout the vertebrate evolution. Accordingly, this region also interacts with cholesterol, its precursor, i.e. mevalonate and its derivatives, namely stigmasterol and aldosterone [3]. This in general suggest that the TM4-Loop-TM5 region of TRPV4 is involved in the interaction of several biomolecules, and thus may act as a molecular sensor for cellular metabolism. Recently, we reported that TRPV4 localizes within mitochondria and interacts with certain mitochondrial proteins, namely with Mfn1, Mfn2 and Cyt C present in the mitochondrial extract [4]. In this work, we explored the direct interaction of Cytochrome C (Cyt C) with the hot-spot region of TRPV4 and factors that can influence such interactions.

2. Material and methods

2.1. Cloning of hTRPV4 fragments, protein expression-purification

hTRPV4 fragment TRPV4 (amino acid 592-630, termed as Fr592-630) and its different point mutants fused with GST (GST-TRPV4-Fr592-630-WT, GST-TRPV4-Fr592-630-R616Q, GST-TRPV4-Fr592-630-F617L, GST-TRPV4-Fr592-630-L618P, and GST-TRPV4-Fr592-630-V620I) were cloned into the BamHI and SalI site of pGEX-6P1 vector, expressed in *Escherichia coli* by IPTG-induction and purified further as described before [5] . The desired fragment was amplified using following primers FP: 5' GTAGGATCCATGTTCACCCGTGGGCTGAAG 3' and RP: 5'-GTTGTCGACTGAAGCGTAGCCGATCATGAA 3'

2.2. GST pull-down assay for identifying V4- Fr592-630 interaction with Cyt C

To explore if TRPV4-Fr592-630 interacts with Cyt C, pull-down experiments were performed using purified monomeric Cyt C (Sigma). TRPV4-Fr592-630 and its mutants were cloned into pGEX-6P1-GST vector and these fusion proteins were expressed in *E. coli*. Only GST was used as a negative control. After expression and purification, GST-tagged proteins were immobilized on Glutathione Sepharose beads for 12 hours at 4°C. Subsequently washed with GST wash buffer (1M Tris-Cl (pH 7.5)-5ml, NaCl-1.5g, 0.5M EDTA-200 µl, EGTA-38mg, H_20-95ml) and 30 µL of Cyt C (50µM protein) were added onto the sepharose beads bound with GST-V4-Fr592-630 or mutant proteins and incubated for 4 hours at 4°C. This experiment was also done in the presence or absence of Cu^{2+}, Fe^{3+}, Mn^{2+}, Ni^{2+} and Zn^{2+} (100µM each). In some experiments, EGTA (5mM) was used to chelate Ca^{2+} present in the buffer. Thereafter, the beads were washed 3 times with GST wash buffer, and all protein/s bound to the beads were eluted in 100 µL of elution buffer (20 mM Glutathione reduced 50 mM Tris-Cl pH 8.0). Eluted samples were further analyzed by SDS–PAGE (12%) followed by Western blot analysis with anti-Cyt C or GST antibodies (Abcam).

2.3. Retrieval of TRPV4 protein sequences

The protein sequence for hTRPV4 (accession no- Q9HBA0) was retrieved from Uniprot. All other protein sequences of TRPV4 and Cytochrome C from different species used in this study were retrieved from either NCBI or Uniprot database (**Supplementary table 1** and **Supplementary table 2**). All the sequences were stored in FASTA format and MUSCLE alignment tool in MEGA 5.1 software suite was used for the alignment of the proteins.

2.4. Docking of Cyt C with TRPV4

Structure of recombinant human Cyt C protein, PDB ID-3ZCF was downloaded from PDB. TRPV4 3D structure was made by homology modelling with *Xenopus tropicalis* as the target structure using YASARA homology modeling module as described before [6] The protein-protein docking was performed using HADDOCK Web Server keeping the default parameters as standard settings.

3. Results

Cyt C and TRPV4 co-localizes within mitochondria

Previously we reported that TRPV4 localizes within mitochondria [7]. Therefore, we explored the co-localization of TRPV4 with Cyt C by immunofluorescence analysis. For that purpose, we used HaCaT cell line, transiently expressed TRPV4, fixed the cells and stained for TRPV4 with a rabbit antibody and endogenous Cyt C with a mouse antibody. Cells were also treated with TRPV4 activator, (i.e., 4αPDD, 1 μM) before fixing. We have noticed co-localization in both cases, though greater colocalization is seen in case of TRPV4-activated condition (**Figure 1a**).

Amino acid 592-630 of TRPV4 interacts with Cyt C in a metal ion-sensitive manner

Bioinformatic prediction results suggest that amino acid 592-630 of TRPV4 has several point mutations within this patch and also has the maximum likelihood for mitochondrial localization. We cloned this fragment as a GST-tagged protein (AA number 592-630 of TRPV4 into pGEX6P1 vector and termed as GST-V4-Fr592-630]. The protein fragment was expressed, purified and subsequently used for pull-down experiments with purified Cyt C. Only GST was used as a negative control. The pull-down samples were probed for the presence of Cyt C by Western Blot analysis. We detect a monomeric band at 14 kDa and often a dimeric band at ~35 kDa, only in the sample that was pulled down using GST-V4-Fr592-630, but not in the pulldown sample that used only GST (**Figure 1b**). This suggests direct interaction of Cyt C with V4-Fr592-630 region.

To further characterize the interaction of Cyt C with V4-Fr592-630, the pull-down experiment was performed with purified Cyt C (oxidised form) in presence of EGTA (Ca^{2+}-chelator) and different concentration of Ca^{2+} (**Figure 1c**). Results suggest that V4-Fr592-630 interacts with Cyt C more in presence of Ca^{2+} in dose-dependent manner. Presence of EGTA (5 mM) decreased (but not abolished) this interaction, suggesting that this interaction is sensitive but not dependent to Ca^{2+}-ions. This interaction was not observed with only GST. Further experiments were performed in presence of other divalent (Cu^{2+}, Mn^{2+}, Ni^{2+} and Zn^{2+}) and trivalent metals (Fe^{3+}). Cyt C interacts with V4- Fr592-630 differently in presence of these metal ions. Such type of interactions was not observed with GST protein (used as negative control). This result implies that Cyt C interaction with V4- Fr592-630 is very specific and this interaction is sensitive to the presence of different metals (**Figure 1d**). Quantification of monomeric, dimeric and total (monomeric + dimeric) band (**Supplementary figure 1**) implies that Cyt C interaction with V4-Fr592-630 is very specific and sensitive to the presence of Ca^{2+} as well as other metal ions.

Identification of critical amino acids involved in Cyt C interaction with TRPV4

To analyze the specific interacting residues of TRPV4 involved in Cyt C interaction, we performed *in silico* global and local docking using HADDOCK2.2 Web Server [8]. We performed global docking using TRPV4 tetramer protein and selected amino acid 470-670 from chain A as active site and Cyt C monomer protein. HADDOCK webserver returned 118 structures in 16 cluster(s). The best structure from the top cluster was taken which is the most reliable according to HADDOCK, with the lowest Z-score of -1.4. The protein-protein docking had a total of 11 hydrogen bonds formed between amino acid Ser 667-Lys 25, Asp 662-Lys 22, Thr 665-Glu 21, Ser-663-Gly 23, Ser 663-Lys 22, Arg 661-Lys 22, Ala-565-Thr 28, Lys 530-Lys 87, Phe 533-Lys 87, Gly 627-Lys 7 and Ser 630-Lys 7 of TRPV4 and Cyt C respectively along with some other hydrophobic interactions. For simplifying purpose, only two H-bonds images are shown in detail that lie near the TM4-Loop-TM5 region of TRPV4 using PyMol visualization interface (**Figure 2a**). Another schematic representation of all possible bonds are depicted using LigPlot (**Supplementary figure 2**) [9]. Next, we performed docking analysis of TRPV4 tetramer with Cyt C dimer. For this purpose, we have taken side-by-side Cyt C monomers and docked them with active site amino acid residues 470-670 of TRPV4 tetramer (**Figure 2b**).

Subsequently, local docking was performed using TRPV4 monomer and selecting AA 592-630 as the active sites, and docked it with Cyt C monomer protein. HADDOCK webserver returned 73 structures in 11 cluster(s). The best structure from the top cluster was taken which is the most reliable according to HADDOCK, with the lowest Z-score of -1.5. The protein-protein docking had a total of 7 hydrogen bonds formed with amino acid Phe 592, Thr-593, Arg-594, Ser-603, Gln-607, Leu 618, and Tyr 621 of V4- Fr592-630 with Met-12, Lys-86, Phe-82, Gly-77, Lys-79, Lys-25, and Lys-22 of Cyt C respectively along with some hydrophobic interactions (**Figure 3**).

The interacting residues which were derived from *in silico* investigation were further analyzed for their evolutionary history. Protein sequences of Cyt C and TRPV4 were collected from several vertebrate species. The Fr592-630 region of hTRPV4 was aligned from other species using the default parameters of MUSCLE in Mega 5 software. Similarly, the human Cyt C sequence from AA 12-86 was aligned with Cyt C of other species. The alignments were further visualized using JalView. The high similarity of these sequence suggests that these regions are highly conserved in vertebrates. The amino acids crucial for interaction are rarely substituted by any other residues suggesting their important role throughout vertebrate evolution (**Supplementary figure 3&4**).

Differential interaction of TRPV4-Fr592-630 (and different mutants) with Cyt C

As the amino acid 592-630 region of TRPV4 is a hotspot of several naturally occurring mutations, we explored if the interaction pattern of Cyt C with V4-Fr592-630 differs in case of Wt or mutants. While

some mutations like R616Q and F617L show drastic changes in Ca^{2+}-bound and unbound state interaction with Cyt C, some other mutations like L618P and V620I seems to be less affected by Ca^{2+} and also bind less intensely with Cyt C (**Figure 4 and Supplementary figure 1**).

Taken together, the results suggest differential interaction of TRPV4 with Cyt C which is sensitive to different metal ions and also depends on the mutations present in the hot-spot region.

4. Discussion

The interaction of metal ions with proteins is important as metal-binding proteins utilize metals for their structure stabilization required for their activity. Interfacial metal ions stabilize permanent or transient protein-protein interactions also, enable protein complexes to adopt distinct conformations and perform specific cellular functions. In this regard, Cyt C represents a metal-binding protein which is very ancient and critical protein involved in several biological functions. So far, more than 70000 cytochromes have been discovered from different biological sources [10]. All these cytochromes have tetrapyrrole ring bound with iron (known as heme-group) at their centre**.** The bound iron atom can fluctuate between the oxidation states Fe^{3+} and Fe^{2+}, so that cytochromes generally function as a one-electron carrier. It transfers electrons in the mitochondrial respiratory chain from cytochrome bc1 complex to cytochrome c oxidase. Due to its property, Cyt C also act as a redox sensor [11]. The heme-moiety of cytochrome c exists in interconvertible reduced (Fe^{2+}) or oxidized (Fe^{3+}) forms that shuttle electrons from Cyt C reductase to Cyt C oxidase [12]. This water-soluble low-molecular-weight (13000 Da; 104 amino acids) protein is known to exist in an aqueous solution as the native monomer as well as a dimer, trimer, and tetramer [13]. In this work, we demonstrate direct binding of Cyt C with a fragment of TRPV4. This interaction is observed for both monomeric as well as dimeric Cyt C (and for higher order complexes in certain cases). For several reasons, TRPV4-Cyt C interaction is very important for physiology and is relevant for diseases.

First, this interaction can be detected in a small region of TRPV4, i.e., amino acid region 592-630 of TRPV4, which also represents the TM4-loop-TM5 region. Sequence analysis suggests that the key amino acids of TRPV4 involved in this interaction are highly conserved throughout the vertebrate evolution. This small region is also a hot-spot for several pathogenic mutations that cause a series of neuronal and muscular disorders commonly known as “TRPV4-mediated channeopathies” [14]. Considering that TRPV4 is also detected in the mitochondria, and interacts with Cyt C, a key mitochondrial protein, it is highly probable that TRPV4-Cyt C complex present in the mitochondria is relevant for diseases. Notably, phenotypes of several mitochondrial disorders are very similar to TRPV4 mutation mediated disorders, suggesting that these mitochondrial and/or metabolic disorders are probably same or at least linked with these TRPV4-

mediated channelopathies. In this context, it is worth to mention that most of these mutations act as "gain-of-function" mutants, causing influx of more metal ions and/or less desensitization. In this notion, interaction of monomeric and dimeric Cyt C with different mutants of TRPV4 strongly suggest that different mutants form complexes that are with different stoichiometry and thus may have different functions and regulations.

Second, we demonstrate that TRPV4-Cyt C interaction varies in presence of different metal ions. The ion-binding properties of Cyt C is of great interest as binding of different ions profoundly affects its reactivity. At least eight ion-binding sites on cytochrome c have been identified and ion-binding properties is relevant for mitochondrial ion transport [15]. It is known that mitochondrial physiology requires transition metal ions, such as Copper, iron, manganese, Nickel and zinc which mostly act as cofactors in metalloenzymes and metalloproteins present there. Notably, Zn^{+2} acts as inhibitor of Cytochrome C oxidase [16]. Therefore, our findings also suggest that TRPV4-Cyt C complex may function as a sensor for different metals present in the local environment. Therefore, differential interaction of TRPV4-Cyt C in response to these different metals are relevant and perturbation in these metal pools inside mitochondria may result in altered activity of TRPV4-Cyt C complex as well as other key enzymes and/or proteins there [17].

Third, the TRPV4-Cyt C complex is sensitive to Ca^{2+}. This aspect might have importance in case of apoptosis. Ca^{2+} is known to be accumulated in the mitochondrial matrix against a concentration gradient. Release of Cyt C from mitochondria in response to increased Ca^{2+}-level in cytosol triggers apoptosis [18]. As TRPV4-activation causes Ca^{2+}-influx, TRPV4 activation can be directly linked with apoptosis. Indeed, importance of TRPV4 in cell death has also been demonstrated [19].

Fourth, interaction of monomeric Cyt C with TRPV4-Fr-592-630 (or different mutants) not only results in formation of complex, but also formation of stable Cyt C dimer, trimer and often tetramer that become resistant in SDS-PAGE. Also, the total extent and relative ration of these monomer with dimer suggests that each mutation has unique properties in terms of TRPV4-Cyt C complex formation.

Taken together, we conclude that a small fragment of TRPV4 interacts with Cyt C. This interaction is highly variable depending on the presence of different metal ions including Ca^{2+}. This interaction is also variable depending on the sequence of TRPV4 and its mutants. These findings may have a strong bio-medical implication. We propose that TRPV4-Cyt C complex is critical for understanding several diseases that represent TRPV4-induced channelopathy and/or mitopathy at molecular and cellular levels.

Acknowledgments:

Funding from NISER and DBT (Govt. India, grant number BT-BRB-TF-2-2011 & BT/PR8004/MED/30/988/2013) are acknowledged. CG acknowledge the previous supports from MPI, Berlin and Dr. A. Santle for help with certain antibodies. CG acknowledges all the present and former lab members for supporting this work.

Author contributions and declaration:

CG conceptualized the project, wrote the grant, provided reagents, facilities for the experiments and provided guidance. RD1, AK and RD2 performed all the experiments, analyzed the data and manuscript preparation. CG edited the final manuscript. All authors declare the existence of no conflict with this work. The funders had no role in study design, data collection and analysis, decision to publish, or preparation of the manuscript.

Reference

[1] A. Ghosh, N. Kaur, A. Kumar, C. Goswami, Why individual thermo sensation and pain perception varies? Clue of disruptive mutations in TRPVs from 2504 human genome data, Channels. 10 (2016) 339–345. https://doi.org/10.1080/19336950.2016.1162365.

[2] B.A. McCray, A. Schindler, J.E. Hoover-Fong, C.J. Sumner, Autosomal dominant TRPV4 disorders, GeneReviews®. (2020) 1–27. http://www.ncbi.nlm.nih.gov/pubmed/24830047.

[3] S. Kumari, A. Kumar, P. Sardar, M. Yadav, R.K. Majhi, A. Kumar, C. Goswami, Influence of membrane cholesterol in the molecular evolution and functional regulation of TRPV4, Biochem. Biophys. Res. Commun. 456 (2015) 312–319. https://doi.org/10.1016/j.bbrc.2014.11.077.

[4] A. Kumar, R. Kumar Majhi, T. Kanta Acharya, K.-H. Smalla, E.D. Gundelfinger, C. Goswami, TRPV4 interacts with mitochondrial proteins and acts as a mitochondrial structure-function regulator, (n.d.). https://doi.org/10.1101/330993.

[5] C. Goswami, J. Kuhn, P.A. Heppenstall, T. Hucho, Importance of Non-Selective Cation Channel TRPV4 Interaction with Cytoskeleton and Their Reciprocal Regulations in Cultured Cells, PLoS One. 5 (2010) e11654. https://doi.org/10.1371/journal.pone.0011654.

[6] R. Das, C. Goswami, Biochemical and Biophysical Research Communications TRPV4 expresses in bone cell lineages and TRPV4-R616Q mutant causing Brachyolmia in human reveals " loss-of-interaction " with cholesterol, Biochem. Biophys. Res. Commun. (2019). https://doi.org/10.1016/j.bbrc.2019.07.042.

[7] A. Kumar, R.K. Majhi, T.K. Acharya, K.-H. Smalla, E.D. Gundelfinger, C. Goswami, TRPV4 interacts with mitochondrial proteins and acts as a mitochondrial structure-function regulator, BioRxiv. (2018) 330993. https://doi.org/10.1101/330993.

[8] G.C.P. Van Zundert, J.P.G.L.M. Rodrigues, M. Trellet, C. Schmitz, P.L. Kastritis, E. Karaca, A.S.J. Melquiond, M. Van Dijk, S.J. De Vries, A.M.J.J. Bonvin, The HADDOCK2.2 Web Server: User-Friendly Integrative Modeling of Biomolecular Complexes, J. Mol. Biol. 428 (2016) 720–725. https://doi.org/10.1016/J.JMB.2015.09.014.

[9] R.A. Laskowski, M.B. Swindells, LigPlot+: Multiple LigandÀProtein Interaction Diagrams for Drug Discovery, J. Chem. Inf. Model. 51 (2011) 2778–2786. https://doi.org/10.1021/ci200227u.

[10] J. Liu, S. Chakraborty, P. Hosseinzadeh, Y. Yu, S. Tian, I. Petrik, A. Bhagi, Y. Lu, Metalloproteins Containing Cytochrome, Iron–Sulfur,or Copper Redox Centers, Chem. Rev. 114 (2014) 4366. https://doi.org/10.1021/CR400479B.

[11] Electron-Transport Chains and Their Proton Pumps - Molecular Biology of the Cell - NCBI Bookshelf, (n.d.). https://www.ncbi.nlm.nih.gov/books/NBK26904/ (accessed March 31, 2022).

[12] G.C. Brown, V. Borutaite, Regulation of apoptosis by the redox state of cytochrome c, Biochim. Biophys. Acta - Bioenerg. 1777 (2008) 877–881. https://doi.org/10.1016/j.bbabio.2008.03.024.

[13] E. MARGOLIASH, J. LUSTGARTEN, Interconversion of horse heart cytochrome C monomer and polymers., J. Biol. Chem. 237 (1962) 3397–3405. https://doi.org/10.1016/s0021-9258(19)70829-1.

[14] P. Verma, A. Kumar, C. Goswami, TRPV4-mediated channelopathies, Channels. 4 (2010) 319–328. https://doi.org/10.4161/chan.4.4.12905.

[15] C.O. AREAN, G.R. MOORE, G. WILLIAMS, R.J.P. WILLIAMS, Ion binding to cytochrome c, Eur. J. Biochem. 173 (1988) 607–615. https://doi.org/10.1111/j.1432-1033.1988.tb14042.x.

[16] S.S. Kuznetsova, N. V. Azarkina, T. V. Vygodina, S.A. Siletsky, A.A. Konstantinov, Zinc ions as cytochrome C oxidase inhibitors: two sites of action, Biochemistry. (Mosc). 70 (2005) 128–136. https://doi.org/10.1007/S10541-005-0091-6.

[17] F. Pierrel, P.A. Cobine, D.R. Winge, Metal Ion availability in mitochondria, BioMetals. 20 (2007). https://doi.org/10.1007/s10534-006-9052-9ï.

[18] C. Garrido, L. Galluzzi, M. Brunet, P.E. Puig, C. Didelot, G. Kroemer, Mechanisms of cytochrome c release from mitochondria, Cell Death Differ. 2006 139. 13 (2006) 1423–1433. https://doi.org/10.1038/sj.cdd.4401950.

[19] A. Olivan-Viguera, A.L. Garcia-Otin, J. Lozano-Gerona, E. Abarca-Lachen, A.J. Garcia-Malinis, K.L. Hamilton, Y. Gilaberte, E. Pueyo, R. Köhler, Pharmacological activation of TRPV4 produces immediate cell damage and induction of apoptosis in human melanoma cells and HaCaT keratinocytes, PLoS One. 13 (2018). https://doi.org/10.1371/JOURNAL.PONE.0190307.

Figures and legends:

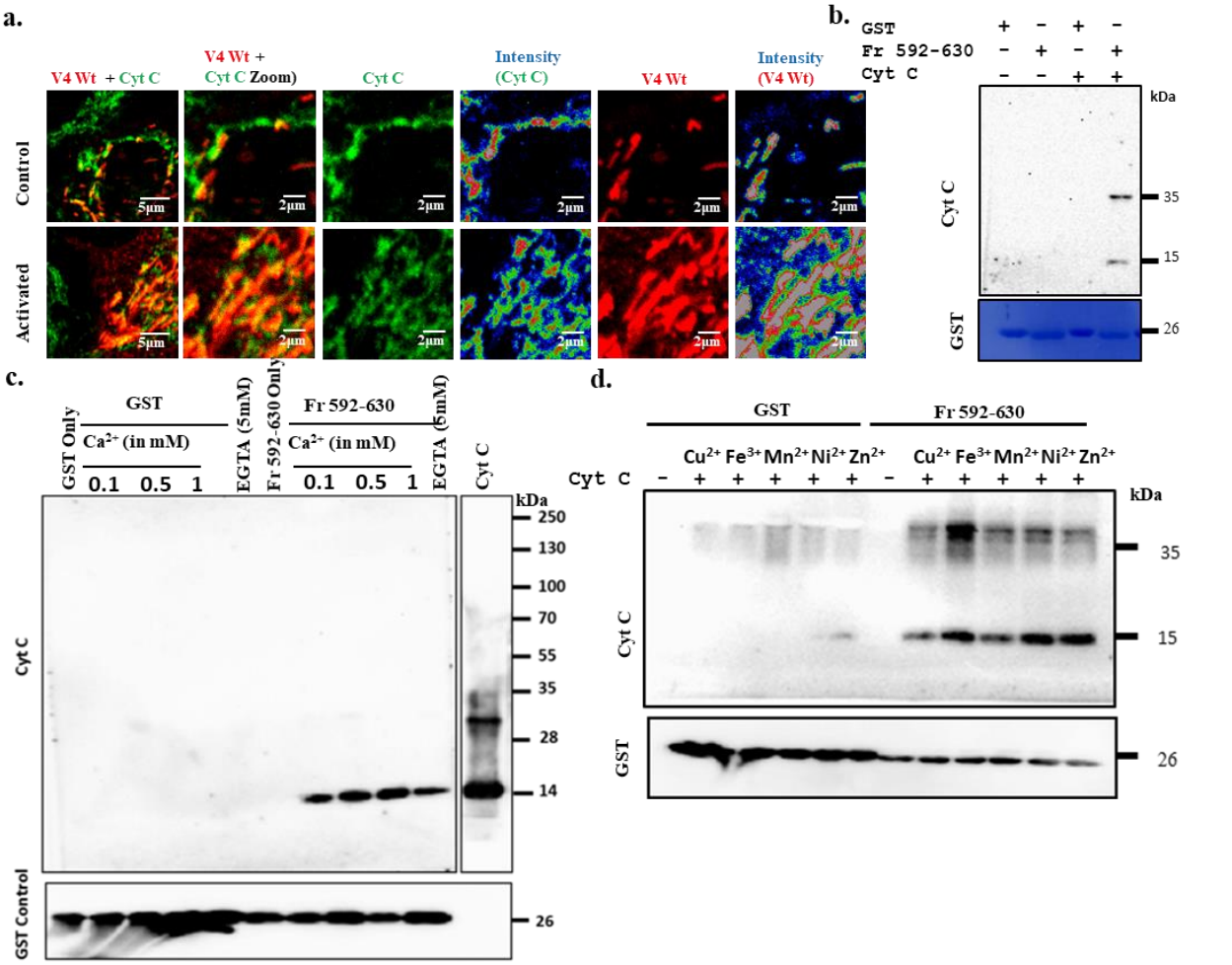

Figure 1: A small fragment of TRPV4 interacts with Cyt C and this interaction differs due to the presence of different metals. a. Confocal images demonstrating the co-localization of TRPV4 with Cyt C within mitochondria. The images depict TRPV4 (red) signal overlaps with Cyt C (green) in control and 4αPDD-treated conditions. Fluorescence intensity from Cyt C and TRPV4 in all cases are represented in pseudo rainbow colour (red and blue represent highest and lowest intensity respectively). **b**. GST-V4-Fr592-630 or GST-only (used as a negative control) were expressed, immobilized on resin-beads and subsequently purified Cyt C was added for interaction studies. All the pulled down samples were probed for western blot analysis using anti-Cyt C antibody. A monomeric Cyt C band (15 kDa) and a dimeric band (near 35 kDa) are observed. Corresponding loading control is shown by Coomassie Brilliant Blue-stained gel. **c.** Experiment as described in b was performed in presence of different amount of Ca^{2+} and its chelator, namely EGTA. This interaction is sensitive to the presence of Ca^{2+}. **d.** Similar pull down experiment was performed in presence of Cu^{2+}, Fe^{3+}, Mn^{2+}, Ni^{2+} or Zn^{2+} independently. Loading amount is detected by Western Blot analysis using GST antibody. For quantification of interaction, kindly see supplementary figure 1.

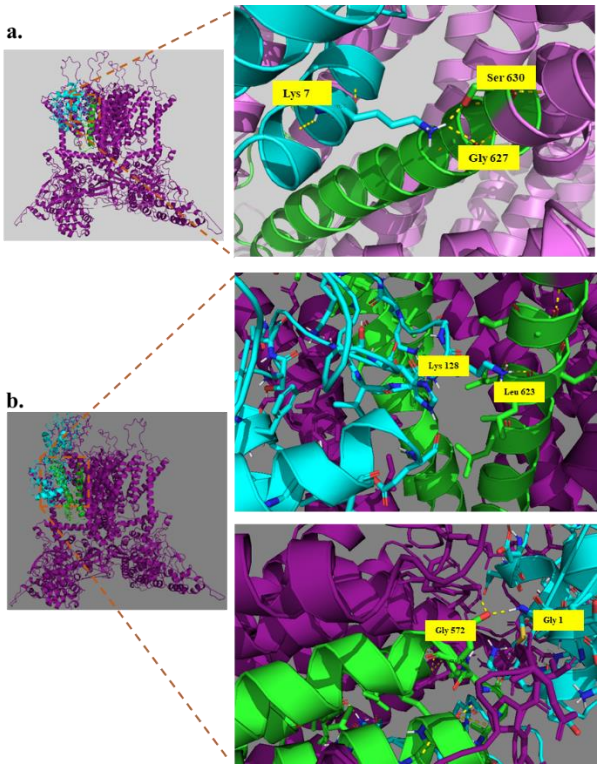

Figure 2: TRPV4 interacts with monomeric and dimeric Cyt C. **a.** *In silico* docking analysis using PyMol illustrates TRPV4 tetramer (purple) interacts with Cyt C monomer (cyan) near the TM5-loop-TM5 region (green) of TRPV4 protein. The enlarged images showing the H-bonds (as yellow dotted lines) and the respective residues (highlighted in yellow). For example, Lysine 7 from Cyt C forms two hydrogen bonds with Serine 630 and Glycine 627 of TRPV4 protein. **b.** TRPV4 interacts with Cyt C dimer *in silico*. A total of 15 H-bonds was found and some selected residues forming the bonds are highlighted in yellow.

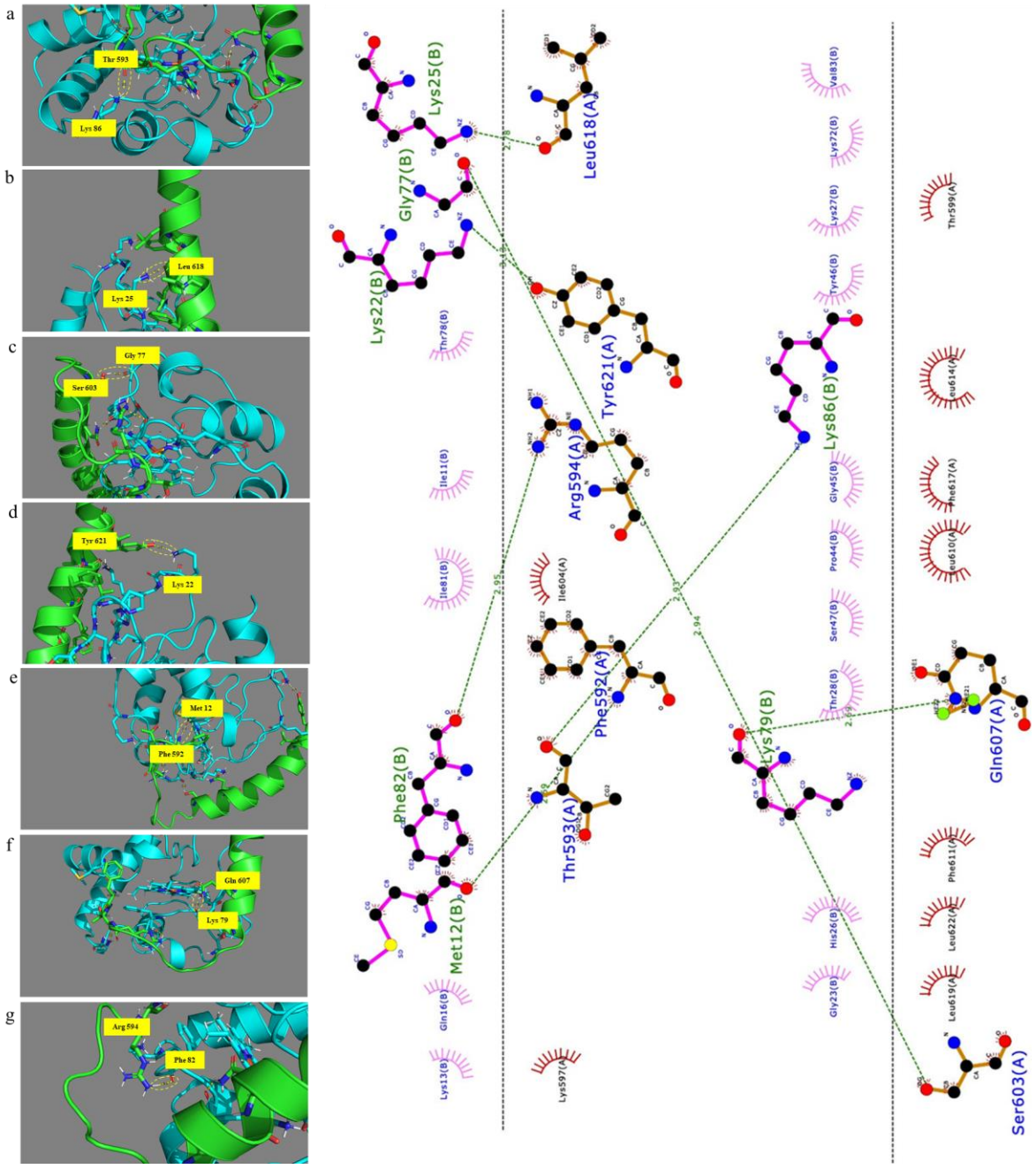

Figure 3: TRPV4 fragment (amino acid592-630) interacts with Cyt C monomer *in silico*. a-g. Docking analysis by PyMol suggests presence of several H-bonds (yellow dotted lines) between V4-Fr592-630 (green) and Cyt C monomer (cyan). Total seven H-bonds were found and the residues forming the bonds are highlighted in yellow. **h.** Analysis using LigPlot provides 2D-schematic diagrams of protein-protein interactions from the 3D co-ordinate files. Presence of several H-bonds and hydrophobic interactions between V4-Fr592-630 (A: blue) and Cyt C (B: green) is detected. Green dotted line: H-bond and its length, Red spiked semicircles: Non ligand residues involved in hydrophobic contacts.

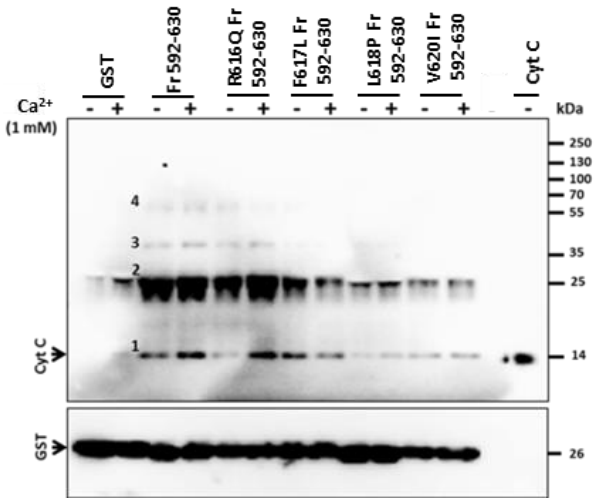

Figure 4: Differential interaction of Cytochrome C with TRPV4 mutants in presence and absence of Ca^{2+}. a. Purified GST-V4-Fr592-630, GST-V4-Fr592-630-R616Q, GST-V4-Fr592-630-F617L, GST-V4-Fr592-630-L618P, GST-V4-Fr592-630-V620I and GST-only were incubated separately on glutathione sepharose beads alone or in presence of Ca^{2+}. Purified Cyt C was added for interaction studies. Western blot analysis using anti-Cyt C antibody detects bands for monomeric, dimeric, trimeric and tetrameric Cytochrome C (shown as 1, 2, 3 & 4). Loading amount is analyzed by western blot staining by GST antibody. For quantification of interaction, kindly see supplementary figure 1.

Supplementary figures

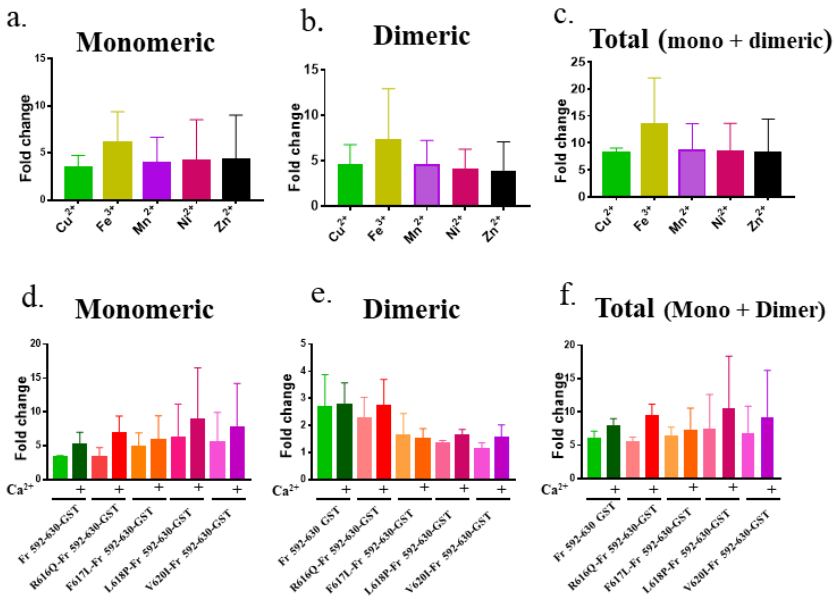

Supplementary figure 1: Quantification of Cytochrome C bands interacting with TRPV4 (in presence of different metal ions) and its mutants. a-c. Quantification of monomeric (**a**), dimeric (**b**) and total (monomer + dimer) (**c**) Cytochrome C suggests that TRPV4 interaction to Cyt C is sensitive to the presence of different metal ions. **d-f.** Quantification of monomeric (**d**), dimeric (**e**), and total (monomer + dimer) (**f**) the band intensity of Cyt C suggests differential interaction pattern of TRPV4 and its mutants with Cyt C.

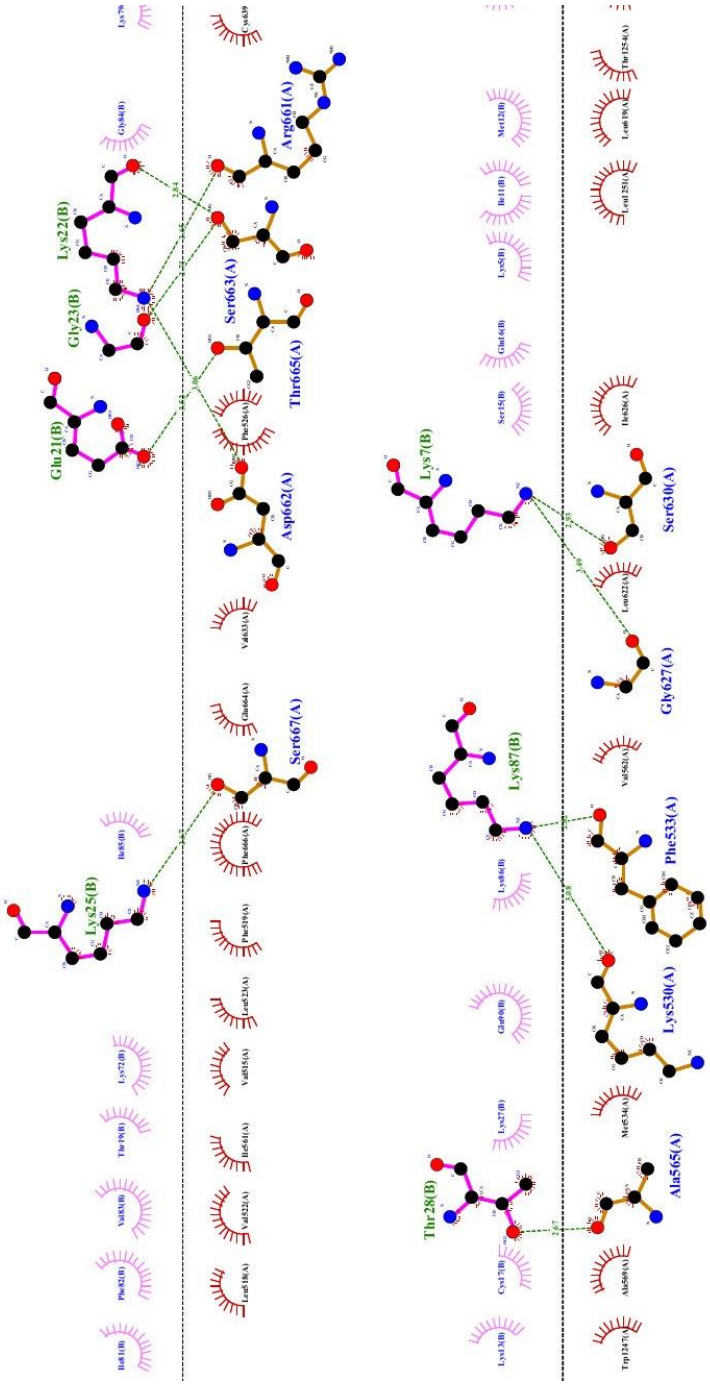

Supplementary figure 2: TRPV4 interacts with Cyt C monomer *in silico*. Analysis using LigPlot provides 2D schematic diagrams of protein-protein interactions from the 3D co-ordinate files. Image suggests presence of several H-bonds and hydrophobic interactions between TRPV4 (A: blue) and Cyt C (B: green). Different bonds are depicted in different colour. Green dotted line: H-bond and its length, Red spiked semicircles: Non ligand residues involved in hydrophobic contacts.

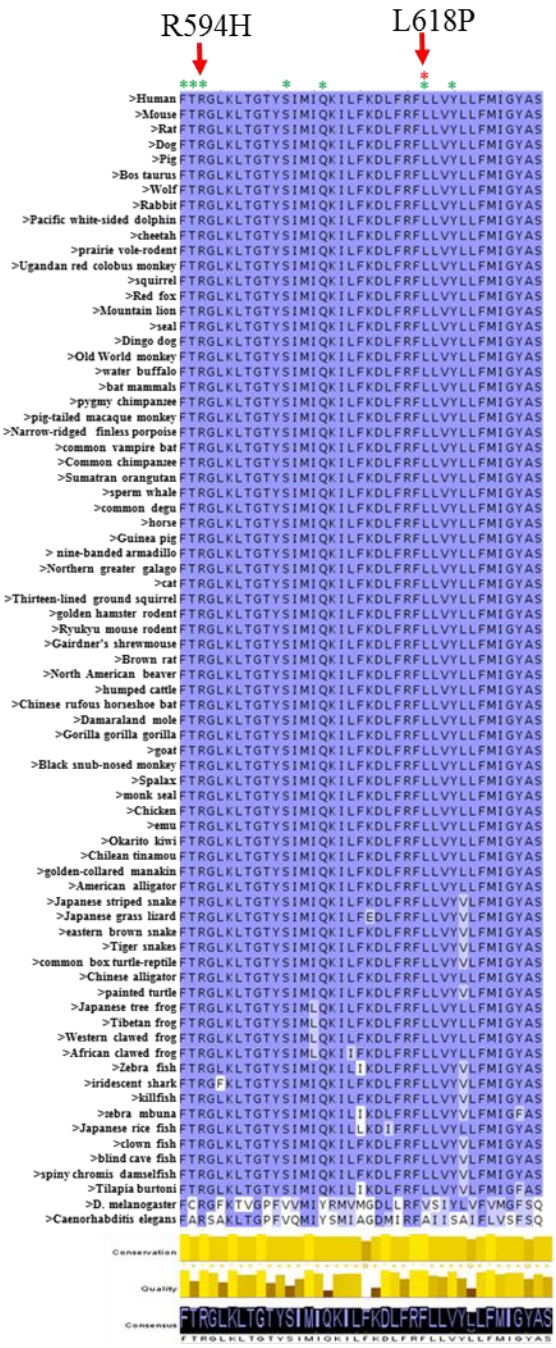

Supplementary figure 3: Conservation of Cyt C interacting residues of TRPV4. Conservation analysis of TRPV4 amino acid sequence 592-630 is shown. The amino acids present in this region are mostly conserved in all vertebrates. The crucial amino acids that interact with Cyt C are indicated with green asterisk (*). Two human mutations occurring positions R594 & L618 are marked in red arrow.

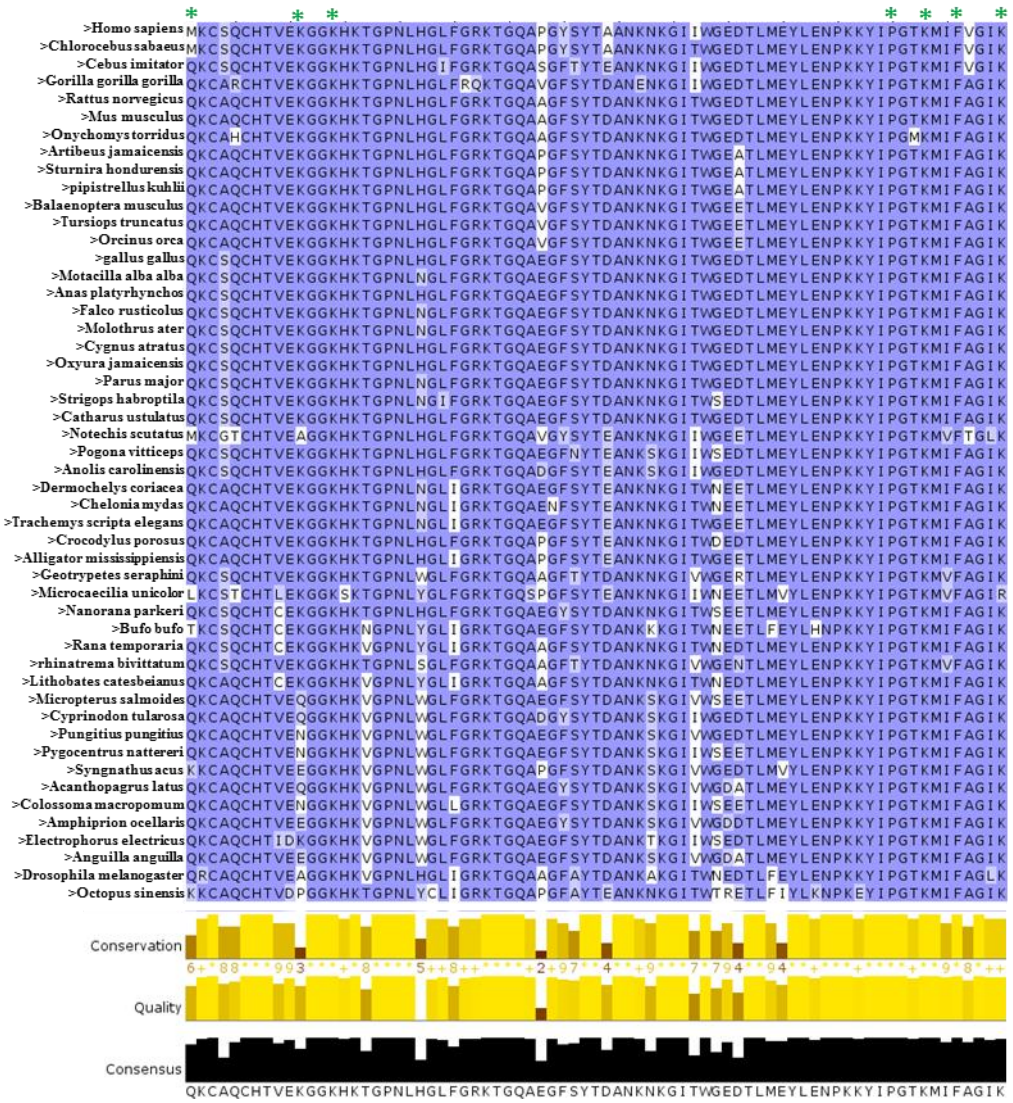

Supplementary figure 4: Conservation of TRPV4 interacting residues of Cyt C. Conservation analysis of Cyt C sequence from amino acid 12-86 is shown. The amino acids present in this region are mostly conserved in all vertebrates. The crucial amino acids that interact with TRPV4 are indicated with green asterisk (*).

Supplementary table 1: Details of TRPV4 sequences used for analysis

Organisms	*Scientific Name*	Protein ID	Length (aa)
Human	*Homo sapiens*	UniProtKB - Q9HBA0	871
Mouse	*Mus musculus*	UniProtKB - Q9EPK8	871
Rat	*Rattus norvegicus*	UniProtKB - Q9ERZ8	871
Dog	*Canis lupus familiaris*	GenBank: ABU40239.1	871
Pig	*Sus scrofa*	NCBI NP_001124201.1	871
Cattle	*Bos taurus*	NCBI :NP_001179314.1	871
Wolf	*Canis lupus familiaris*	NCBI:NP_001120787.1	871
Rabbit	*Oryctolagus cuniculus*	GenBank: AOV86376.1	866
Pacific white-sided dolphin	*Lagenorhynchus obliquidens*	NCBI: XP_026980306.1	870
Cheetah	*Acinonyx jubatus*	NCBI:XP_026899867.1	871
Prairie vole	*Microtus ochrogaster*	NCBI:XP_005344323.1	871
Squirrel	*Urocitellus parryii*	NCBI: XP_026264981.1	871
red fox	*Vulpes vulpes*	NCBI : XP_025842436.1	868
mountain lion	*Puma concolor*	NCBI: XP_025789376.1	867
seal mammal	*Callorhinus ursinus*	NCBI : XP_025745161.1	871
Dingo Dog	*Canis lupus dingo*	NCBI : XP_025330048.1	871
Old World monkey	*Theropithecus gelada*	NCBI : XP_025257875.1	871
water buffalo	*Bubalus bubalis*	NCBI : XP_025123264.1	871
Bat	*Pteropus alecto*	NCBI : XP_015452796.1	875
pygmy chimpanzee	*Pan paniscus*	NCBI : XP_008956168.1	871
pig-tailed macaque monkey	*Macaca nemestrina*	NCBI : XP_011759392.1	871
common vampire bat	*Desmodus rotundus*	NCBI : XP_024422550.1	870
Common chimpanzee	*Pan troglodytes*	NCBI : XP_016779641.1	871
Sumatran orang-utan	*Pongo abelii*	NCBI : XP_024113283.1	871
sperm whale	*Physeter catodon*	NCBI : XP_007115658.2	871
common degu	*Octodon degus*	NCBI : XP_023576734.1	871
Guinea pig	*Cavia porcellus*	NCBI : XP_003477960.1	871
nine-banded armadillo	*Dasypus novemcinctus*	NCBI : XP_004478492.1	871
Northern greater galago	*Otolemur garnettii*	NCBI : XP_012660746.1	870
Cat	*Felis catus*	NCBI: XP_023097285.1	871
Thirteen-lined ground squirrel	*Ictidomys tridecemlineatus*	NCBI : XP_005340170.1	871
golden hamster	*Mesocricetus auratus*	NCBI : XP_012975259.1	870
Ryukyu mouse	*Mus caroli*	NCBI: XP_021017792.1	871
Gairdner's shrewmouse	*Mus pahari*	NCBI : XP_021078175.1	870
Brown rat	*Rattus norvegicus*	NCBI : XP_006249528.1	871
North American beaver	*Castor canadensis*	NCBI : XP_020021894.1	871

humped cattle	*Bos indicus*	NCBI : XP_019833659.1	871
Chinese rufous horseshoe bat	*Rhinolophus sinicus*	NCBI : XP_019613090.1	871
Damaraland mole	*Fukomys damarensis*	NCBI : XP_010602262.1	871
Gorilla	*Gorilla gorilla gorilla*	NCBI : XP_018894818.1	871
Goat	*Capra hircus*	NCBI : XP_017916595.1	871
Black snub-nosed monkey	*Rhinopithecus bieti*	NCBI: XP_017735181.1	871
Spalax	*Nannospalax galili*	NCBI : XP_017657653.1	871
monk seal	*Neomonachus schauinslandi*	NCBI : XP_021559167.1	871
Chicken	*Gallus gallus*	UniProtKB - A0A1D5PXA5	852
Emu	*Dromaius novaehollandiae*	NCBI : XP_025970319.1	858
Chilean tinamou	*Nothoprocta perdicaria*	NCBI : XP_025892494.1	846
golden-collared manakin	*Manacus vitellinus*	NCBI : XP_017931657.1	894
American alligator	*Alligator mississippiensis*	NCBI : NP_001304074.1	857
Japanese striped snake	*Elaphe quadrivirgata*	GenBank: BAK64200.1	868
Japanese grass lizard	*Takydromus tachydromoides*	GenBank: BAK64199.1	868
eastern brown snake	*Pseudonaja textilis*	NCBI : XP_026575079.1	869
Tiger snakes	*Notechis scutatus*	NCBI : XP_026541264.1	868
common box turtle	*Terrapene mexicana triunguis*	NCBI : XP_026512671.1	869
Chinese alligator	*Alligator sinensis*	NCBI : XP_025055210.1	865
painted turtle	*Chrysemys picta bellii*	NCBI : XP_023957245.1	869
Japanese tree frog	*Dryophytes japonicus*	GenBank: BAN04747.1	871
Tibetan frog	*Nanorana parkeri*	NCBI : XP_018416484.1	870
Western clawed frog	*Xenopus tropicalis*	UniProtKB - F7BWY7	868
African clawed frog	*Xenopus laevis*	UniProtKB - A0A1L8HQ36	868
Zebra fish	*Danio rerio*	NCBI : NP_001036195.1	841
iridescent shark	*Pangasianodon hypophthalmus*	NCBI : XP_026767179.1	854
Killfish	*Kryptolebias marmoratus*	NCBI : XP_017269494.1	873
zebra mbuna	*Maylandia zebra*	NCBI : XP_004544601.1	873
Japanese rice fish	*Oryzias latipes*	NCBI : XP_020561608.1	871
clown fish	*Amphiprion ocellaris*	NCBI : XP_023125651.1	873
blind cave fish	*Astyanax mexicanus*	NCBI : XP_022521975.1	866
spiny chromis damselfish	*Acanthochromis polyacanthus*	NCBI: XP_022054098.1	873
Tilapia burtoni	*Haplochromis burtoni*	NCBI : XP_014194860.1	873
Fruit fly	*D. melanogaster*	FBpp0088509 NAN protein	833
Round worm	*Caenorhabditis elegans*	OSM-9 B0212.5	937

Supplementary table 2: Details of Cytochrome C sequences used for analysis

Species Name	Identifier	Sequence	Accession No.	Family
Homo sapiens	Human	105	NP_061820.1	Primates, mammals
Chlorocebus sabaeus	Green Monkey	105	XP_037860678.1	Primates, mammals
Cebus imitator	Panamanian white-faced capuchin	105	XP_017370932.1	Primates, mammals
Gorilla gorilla gorilla	Gorilla	105	XP_018877427.1	Primates, mammals
Rattus norvegicus	brown rat	105	AAA21711.1	Mammals
Mus musculus	house mouse	105	AEP27246.1	Mammals
Onychomys torridus	southern grasshopper mouse	105	XP_036037157.1	Mammals
Artibeus jamaicensis	Jamaican fruit bat	105	XP_036982465.1	Mammals
Sturnira hondurensis	Honduran Yellow-shouldered Bat	105	XP_036897172.1	Mammals
pipistrellus kuhlii	Kuhl's pipistrelle	105	XP_036309633.1	Mammals
Balaenoptera musculus	blue whale	105	XP_036720044.1	Mammals
Tursiops truncates	Bottlenose dolphins	105	XP_033718988.1	Mammals
Orcinus orca	killer whale	105	XP_033276456.1	Mammals
gallus gallus	red junglefowl	105	NP_001072946.1	Birds
Motacilla alba alba	white wagtail	105	XP_037985135.1	Birds
Anas platyrhynchos	mallard	105	XP_027303674.1	Birds
Falco rusticolus	gyrfalcon	105	XP_037241685.1	Birds
Molothrus ater	brown-headed cowbird	105	XP_036261890.1	Birds
Cygnus atratus	black swan	105	XP_035412401.1	Birds
Oxyura jamaicensis	ruddy duck	105	XP_035174113.1	Birds
Parus major	great tit	105	XP_015475502.1	Birds
Strigops habroptila	kakapo	104	XP_030341866.1	Birds
Catharus ustulatus	Swainson's thrush	104	XP_032929801.1	Birds
Notechis scutatus	Tiger snakes	105	XP_026529406.1	Reptiles
Pogona vitticeps	central bearded dragon	105	XP_020636559.1	Reptiles
Anolis carolinensis	green anole	105	XP_003222080.1	Reptiles
Dermochelys coriacea	leatherback sea turtle	174	XP_038249084.1	Reptiles
Chelonia mydas	green sea turtle	163	XP_007071622.2	Reptiles

Trachemys scripta elegans	red-eared slider	105	XP_034616545.1	Reptiles
Crocodylus porosus	saltwater crocodile	105	XP_019390384.1	Reptiles
Alligator mississippiensis	American alligator	129	KYO26818.1	Reptiles
Geotrypetes seraphini	Gaboon caecilian	105	XP_033794803.1	Amphibian
Microcaecilia unicolor	Microcaecilia unicolor	105	XP_030058002.1	Amphibian
Nanorana parkeri	High Himalaya frog	105	XP_018429577.1	Amphibian
Bufo bufo	common toad	105	XP_040289562.1	Amphibian
Rana temporaria	common frog	105	XP_040208820.1	Amphibian
rhinatrema bivittatum	two-lined caecilian	105	XP_029461741.1	Amphibian
Lithobates catesbeianus	American bullfrog	105	ACO51922.1	Amphibian
Micropterus salmoides	largemouth bass	104	XP_038587732.1	Fishes
Cyprinodon Tularosa	White Sands pupfish	104	XP_038132679.1	Fishes
Pungitius pungitius	ninespine stickleback	104	XP_037321857.1	Fishes
Pygocentrus nattereri	red-bellied piranha	104	XP_017559126.1	Fishes
Syngnathus acus	greater pipefish	104	XP_037128136.1	Fishes
Acanthopagrus latus	yellowfin seabream	104	XP_036980575.1	Fishes
Colossoma macropomum	tambaqui	104	XP_036425822.1	Fishes
Amphiprion ocellaris	ocellaris clownfish	104	XP_023150203.1	Fishes
Electrophorus electricus	electric eel	104	XP_026874491.1	Fishes
Anguilla Anguilla	European eel	104	XP_035266771.1	Fishes
Drosophila melanogaster	Fruit fly	108	AAA28437.1	Invertebrates
Octopus sinensis	common octopus	109	XP_029642027.1	Invertebrates

Declaration

All authors declare the existence of no conflict with this work. The funders had no role in study design, data collection and analysis, decision to publish, or preparation of the manuscript.